Notch1 Drives the Formation and Proliferation of Intrahepatic Cholangiocarcinoma*

Jun GUO[1], Wen FU[1], Ming XIANG[1], Yu ZHANG[1], Ke ZHOU[1], Chuan-rui XU[1], Lei LI[1], Dong KUANG[2], Feng YE[3#]
[1]School of Pharmacy, Tongji Medical College, Huazhong University of Science and Technology, Wuhan 430030, China
[2]Department of Pathology, [3]Department of Pediatrics, Tongji Hospital, Tongji Medical College, Huazhong University of Science and Technology, Wuhan 430030, China

Summary: The molecular mechanisms underlying the development of intrahepatic cholangiocarcinoma (ICC) are not clear yet. In this study, we investigated the involvement of Notch1 in the development of ICC. The cDNA microarray analysis showed that Notch1 expression was higher in ICC tissues than in normal biliary epithelial cells. Stable transfection of Notch1 receptor intracellular domain (NICD1) by hydrodynamic tail vein injection induced ICC formation in mice. Western blotting confirmed that Notch1 signaling was activated in human ICC cell lines and mouse ICC tissues. Silencing Notch1 with specific short interfering RNA (siRNA) inhibited the proliferation of ICC cells. Flow cytometry and Western blotting indicated that apoptosis was induced in Notch1-silenced ICC cells compared with controls. Additionally, Notch1 silencing was associated with the inhibition of hairy and enhancer of split-1 (Hes1) and activation of the phosphatase and tensin homolog (PTEN)/p53 pathway. Taken together, these data suggest that Notch1 drives ICC formation and proliferation; downregulation of Notch1 induces apoptosis in ICC cells; Notch1 signaling may serve as a novel therapeutic target for the treatment of ICC.
Key words: Notch1; hydrodynamic transfection; intrahepatic cholangiocarcinoma

Primary liver cancer is one of the most common malignant tumors of the digestive system. According to the 2015 statistics, the incidence of liver cancer ranks the fifth among all cancers[1]. Cholangiocarcinoma (CC) is a major type of liver cancer. It is of malignant nature and can be divided into terminal, perihepatic and intrahepatic CC (ICC)[2, 3].

ICC usually originates from intrahepatic bile duct epithelial cells, and accounts for about 10%–15% of the primary liver malignancies[4, 5]. The five-year survival of patients with ICC is very poor[3, 6]. Patients with ICC are not sensitive to systemic chemotherapy and radiation therapy; the most common treatment is surgical resection[7, 8]. However, due to the long-term asymptomatic progression of ICC, patients are usually diagnosed at a late stage of the disease and are not amenable to surgical treatment[3]. To develop potentially effective treatment regimens, scientists have been attempting to clarify the molecular mechanisms involved in the development of ICC.

Notch1, one of the four receptors of the Notch family, is a ligand-activated transmembrane receptor, which governs differentiation stimulated by direct cell-cell contact in many tissues[9–11]. The function of Notch1 signaling has been studied in the intestinal epithelium of mice deficient in hairy and enhancer of split-1 (Hes1), whose activation leads to the loss of Notch1 signaling and the increase in the number of goblet cells and endocrine cells, along with the decrease in the number of absorptive epithelial cells[12]. Many studies have suggested the association between the Notch1 signaling pathway and several malignancies, as well as the role of Notch1 signaling in angiogenesis, neurogenesis and homeostasis[13, 14].

Primary HCC can be established in mice by chemical or dietary induction, xenotransplantation, or use of transgenic mice[15–17]. However, these methods failed to induce ICC in mouse livers. We previously developed a new method to induce ICC in mice: hydrodynamic transfection of oncogenes[18]. Using different combinations of oncogenes highly expressed in clinical ICC specimens, we established an ICC mouse model that could ideally mimick the genetic alteration and pathological hallmarks of ICC. Biliary manifestations were observed in mouse livers with tumors. The gallbladder and the bile duct were dilated, and the livers were filled with bile-like transparent bubbly liquid. Notably, hematoxylin/

Jun GUO, E-mail: D201881329@hust.edu.cn
#Corresponding author, E-mail: doctoryf@126.com
*This work was supported by the National Natural Science Foundation of China (No. 81801621, No. 81572723, No. 81872253).

eosin (H&E) staining demonstrated the features of human ICC in sections from mice in the Notch1 receptor intracellular domain (NICD1)-injected group. Immunohistochemistry indicated that cytokeratin 19 (CK19), a biomarker of human ICC, was significantly expressed in the tumor tissues relative to the adjacent non-tumor tissues.

In our study, we attempted to investigate the role of Notch1 in driving ICC formation and proliferation, using hydrodynamic transfection method. We also analyzed the effect of knocking down Notch1 on ICC cell proliferation and the underlying molecular mechanism.

1 MATERIALS AND METHODS

1.1 Gene Microarray of Human ICC Samples

The gene microarray results analyzed were from the GEO database (https://www.ncbi.nlm.nih.gov/geo/query/acc.cgi?acc=GSE32225). Human ICC samples from 149 patients were analyzed and 6 lines of normal biliary epithelial cells used as control.

1.2 Construction of NICD1 and Transposase Plasmid

The mouse NICD1 sequence with a Myc tag was cloned into the pT3-EF1α downstream of the EF1α promoter. The hyperactive Sleeping Beauty transposase was expressed from the cytomegalovirus (CMV) promoter as described previously[19].

1.3 Human ICC Samples

Thirty formalin-fixed, paraffin-embedded ICC samples were harvested. All tissues were surgically resected, snap frozen in liquid nitrogen within 0.5 h after the resection, and stored at –80°C. In most cases, both tumor and adjacent non-tumor tissues were collected. A portion of each specimen, 0.5–1 cm^3, was sampled. Each sample was dissected into three equal slices. One was used for RNA extraction, one for protein isolation, and the remaining processed for histological examination. All ICC specimens were from the Department of Pathology, Tongji Hospital (Wuhan, China). Informed consent was acquired from patients before the surgery.

1.4 Hydrodynamic Injection and Mouse Monitoring

FVB/N mice were purchased from the Beijing Vital River Laboratory Animal Technology (China). Hydrodynamic injection was performed as previously described[20]. Twenty-five micrograms of the plasmids encoding pT3-EF1α-NICD1 or pT3-EF1α (the control group) and the Sleeping Beauty transposase (at a ratio of 25:1) were diluted in 2 mL saline (0.9% NaCl) and the solution was filtered using a 0.22-μm filter, then the solution was injected into the lateral tail vein of 6-to-8 weeks old mice in 5–7 s. All animal experiments were approved by the Animal Care and Use Committee, Huazhong University of Science and Technology (China).

1.5 Cell Culture and Transfection

QBC-939 and RBE cells (ATCC, USA) were cultured in RPMI 1640 medium (Hyclone, USA) containing 10% fetal bovine serum (FBS) (HyClone, USA), 100 U/mL penicillin/100 μg/mL streptomycin sulfate (Sigma-Aldrich, USA) and 5 μg/mL plasmocin (Sigma-Aldrich, USA). Notch1 siRNA (stB0007279c-1-5) and scrambled siRNA (stQ0007279-1) were purchased from RIBOBIO (China) and transfected into cells using Lipofectamine 2000 (Invitrogen, USA).

1.6 Colony Formation Assay

In total, 5000 cells were cultured in RPMI 1640 supplemented with 10% FBS, 100 U/mL penicillin G/100 μg/mL streptomycin sulfate, and 5 μg/mL plasmocin (Sigma-Aldrich, USA). Cells were cultured for 14 days at 37°C in an atmosphere of 5% CO_2 and 95% air, fixed with 4% paraformaldehyde for 30 min and washed with phosphate-buffered saline (PBS) three times. Crystal violet was used to dye the cells (incubation: 30 min). The number of colonies over 50 μm in diameter (about 100 cells) in each dish was counted. The assay was repeated three times with duplicate samples.

1.7 Apoptosis Analysis by Flow Cytometry

For fluorescent activated cell sorting (FACS) analysis, ICC cells were treated with Notch1 siRNA for 48 h. Then, both attached and detached cells were harvested and stained using an Annexin V-FITC/PI apoptosis kit (Beyotime, Inc., China) according to the manufacturer's directions. Cells were washed twice with PBS and resuspended in binding buffer, stained with fluorescein isothiocyanate (FITC)/Annexin V for 15 min and with propidium iodide (PI) for 5 min. Flow cytometry analysis was performed on a FACS Calibur (Becton Dickinson, USA). For each sample, a minimum of 10 000 cells were analyzed.

1.8 Protein Extraction and Western Blotting

Mouse liver specimens and ICC cells were homogenized in lysis buffer [30 mmol/L Tris (pH 7.5), 150 mmol/L NaCl, 1% NP-40, 0.5% Na deoxycholate, 0.1% sodium dodecyl sulfate (SDS), 10% glycerol, and 2 mmol/L ethylenediaminetetraacetic acid (EDTA)] containing the Complete Protease Inhibitor Cocktail (Roche Molecular Biochemicals, USA). Protein concentrations were determined with the Bio-Rad Protein Assay Kit (Bio-Rad, USA) using bovine serum albumin as a standard. Protein aliquots (40 μg) were denatured in Tris-Glycine SDS Sample Buffer (Invitrogen, USA), separated by SDS-polyacrylamide gel electrophoresis (PAGE) and transferred to polyvinylidene fluoride (PVDF) membranes. The PVDF membranes were then blocked in 5% milk for 1 h and probed with specific primary antibodies. Antibodies against Notch1 (1:1000), NICD1 (1:1000), Hes1 (1:1000), p53 (1:1000) and cleaved caspase 3 (1:1000) were purchased from

Cell Signaling Technology (USA). Bax (1:1000), Bcl2 (1:1000), phosphate and tension homology (PTEN, 1:1000), murine double minute 2 (MDM2, 1:1000) and α-tubulin antibody were purchased from Proteintech Group (China). Secondary antibody (goat anti-rabbit IgG or goat anti-mouse IgG) (1:2000 dilution; Beijing Zhongshan Golden Bridge Biotechnology Co., Ltd., China) was used. Immunoreactive bands were detected using the chemiluminescence solvent (Thermo Scientific, USA) and visualized with Micro Chemi (DNR Bio-Imaging Systems, Israel).

1.9 Immunohistochemistry

Tumors were collected from the mice after their sacrifice and rinsed in 4% cold paraformaldehyde. Fixed tissue samples were embedded in paraffin, cut into slides, and stained with H&E or subjected to immunohistochemistry or immunofluorescence. For immunohistochemical staining, tumor tissues were fixed in 4% paraformaldehyde overnight at 4°C, treated with ethanol overnight at 4°C and embedded in paraffin blocks. Paraffin slides were dewaxed with xylene, rehydrated through a series of washes with progressively lower percentage of ethanol. Antigen retrieval was performed in 10 mmol/L sodium citrate buffer (pH 6.0) in a microwave on high for 10 min, followed by a 20-min cool down at room temperature. After blocking with the 5% goat serum and avidin-biotin blocking kit (Vector Laboratories, USA), the slides were incubated with the following antibodies: anti-CK19 (CST, USA; 1:100, overnight at 4°C) and anti-Notch1 (CST, USA; 1:100, overnight at 4°C). Slides were then treated with 3% hydrogen peroxide for 10 min to quench endogenous peroxidase activity and then with a biotin-conjugated secondary antibody (Beijing Zhongshan Golden Bridge Biotechnology Co., Ltd., China) (1:400, for 30 min at room temperature). Detection of immunogenic signals was performed with the ABC-Elite Peroxidase Kit (Vector Laboratories, USA) using the DAB Substrate Kit (DakoCytomation, USA).

1.10 Immunofluorescence

Cells were cultured on chamber slides (BD, USA) and fixed with 4% paraformaldehyde containing 0.5% Triton-X100 (Sigma, UK) for 20 min. Then, cells were incubated with appropriate primary antibodies and a fluorescent secondary antibody (Alexa Fluor, Invitrogen). Anti-Notch1 antibody (CST, USA) was used as 1:50 .

1.11 Determination of Liver Function Using Mouse Serum

Serum alanine aminotransferase (ALT), aspartate aminotransferase (AST) and bilirubin were determined enzymatically using the Spinreact Diagnostics Kits (Santa Coloma, Spain) according to the manufacturer's instructions.

1.12 Real-time PCR

Total RNA from mouse liver was extracted using RNeasy Kits (Qiagen, Germany). cDNA was synthesized using the iScript cDNA Synthesis Kit (Bio-Rad, USA). Quantitative values were calculated by using the PE Biosystems Analysis software (Applied Biosystems, USA) using the $2^{\Delta\Delta Ct}$ method[21]; 18s was used as the reference. The primer pairs used are listed in table 1.

Table 1 Primers used for qRT–PCR

Gene		Sequence	Species
GAPDH	F	5'-TGTGGGCATCAATGGATTTGG-3'	Human
	R	5'-ACACCATGTATTCCGGGTCAAT-3'	Human
GAPDH	F	5'-AATGGATTTGGACGCATTGGT-3'	Mouse
	R	5'-TTTGCACTGGTACGTGTTGAT-3'	Mouse
Notch1	F	5'-GAGGCGTGGCAGACTATGC-3'	Human
	R	5'-CTTGTACTCCGTCAGCGTGA-3'	Human
NICD1	F	5'-CCCTTGCTCTGCCTAACGC-3'	Mouse
	R	5'-GGAGTCCTGGCATCGTTGG-3'	Mouse
p53	F	5'-AACTGCGGGACGAGACAGA-3'	Human
	R	5'-AGCTTCAAGAGCGACAAGTTTT-3'	Human
Bax	F	5'-CATATAACCCCGTCAACGCAG-3'	Human
	R	5'-GCAGCCGCCACAAACATAC-3'	Human

F: forward; R: reverse

1.13 Statistical Analysis

All data were analyzed with the Prism 6 software (GraphPad, USA). Comparisons between two groups were performed with two-tailed unpaired or paired *t*-test. Statistical differences among the various groups were assessed with the Tukey Kramer's test. In all histograms, data were presented as mean ± standard error of the mean (SEM).

2 RESULTS

2.1 Overexpression of Notch1 in Human ICC Samples

To determine the expression of Notch1 in human ICC, we examined Notch1 mRNA expression in the GEO database (https://www.ncbi.nlm.nih.gov/geo/query/acc.cgi?acc=GSE32225). The results indicated that Notch1 mRNA was highly expressed in ICC samples as compared with normal biliary epithelial cells (fig. 1A). We then detected the levels of Notch1 protein in 30 human primary ICC samples by immunohistochemistry. We found that Notch1 was significantly expressed in ICC tissues as compared with the adjacent tissues, and it was localized in the nuclei of ICC cells (fig. 1B). Quantitative PCR (qPCR) and Western blotting confirmed that Notch1 mRNA and protein were significantly increased in human ICC tissues (fig. 1C and 1D).

2.2 NICD1-induced Primary ICC in FVB/N Mice

Notch signaling is activated when a ligand binds to a Notch receptor. Upon activation, the Notch receptors are cleaved by disintegin and metalloprotease (ADAM) and γ-secretase. As a result, NICD is released and then translocates into the nucleus and functions as a transcription factor[22]. To explore whether activation of

Notch1 signaling could induce ICC formation in mouse liver, we cloned NICD1, the intracellular domain of Notch1, into the pT3-EF1α vector with a Myc tag (fig. 2A). Then, we transfected NICD1/pT3-EF1α into 293T cells. The qPCR, immunofluorescence, and Western blotting indicated that NICD1 was expressed in 293T cells both at the mRNA (fig. 2B) and protein levels (fig. 2C and 2D).

Next, we injected NICD1/pT3-EF1α and pCMV-SB plasmids into FVB/N mice through the hydrodynamic tail vein injection (fig. 2E). Sleeping beauty transposase could aid the NICD1/pT3-EF1α to integrate into chromosomes of mouse hepatocytes and hence maintain its stable expression. By 18 weeks post injections, tumors were found formed on the surface of mouse livers by palpation. Twenty-one weeks post injection, all mice injected with NICD1/pT3-EF1α and pCMV-SB had tumors formed on the surface of livers. In contrast, tumors were not observed in the livers of the control group. Additionally, the liver volume was significantly greater in the NICD1-injected mice than in the controls (fig. 2F). Biliary manifestations were observed in livers with tumors. The gallbladder and the bile duct were dilated, and the liver was filled with bile-like transparent bubbly liquid.

2.3 Characterization of NICD1-induced ICC in FVB/N Mice

The body weight and body weight/liver weight ratio indicated that the livers in the NICD1-injected group were heavier than those in the control group (fig. 3A). The ALT ratio and bilirubin levels were increased in livers with tumors, showing that liver function was impaired after tumor formation (fig. 3B). Notably, H&E staining demonstrated the features of human ICC in the NICD1-injected group. Immunohistochemistry indicated that CK19, a biomarker of human ICC, was significantly expressed in the tumors rather than in adjacent non-tumor tissues (fig. 3C). qPCR and Western blotting also indicated Notch1 was highly expressed in tumor tissues (fig. 3D–3F). These data collectively indicated that NICD1 expression in mouse liver induced ICC formation.

2.4 Activation of Notch1 Signaling in ICC Cells and Tissues

It has previously been established that, upon activation, Notch1 is cleaved and the released NICD1 translocates to the nucleus and activates Hes1 expression[23]. To explore Notch signaling in ICC, we transfected NICD1 into QBC-939 and RBE ICC cells. Western blotting indicated that NICD1 was highly expressed in cells transfected with NICD1 compared with control cells (fig. 4A and 4B). Correspondingly, the levels of Hes1 increased. Similarly, NICD1 and Hes1 expression increased in ICC tissues of mice injected with NICD1 (fig. 4C and 4D). Based on these observations, we speculated that activation of Notch1

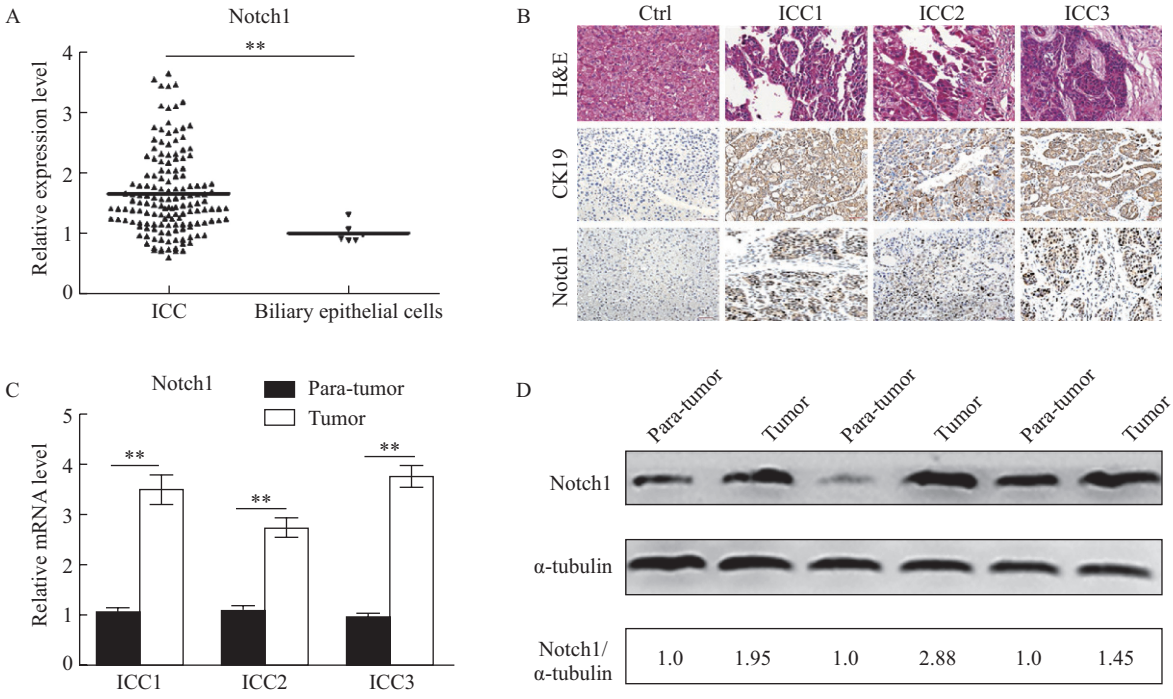

Fig. 1 Notch1 expression in human ICC samples

A: Expression levels of Notch1 in ICC tumors and biliary epithelial cells, which were analyzed using data from GEO database; B: Notch1 protein expression in human tumor tissues and adjacent non-tumor tissues (n=30), as determined by immunohistochemistry (magnification, ×200); C and D: relative expression of Notch1 in human tumor tissues and adjacent non-tumor tissues determined by qPCR (C) and Western blotting (D). Data represent the mean ± SEM of three independent experiments. $^{**}P<0.01$

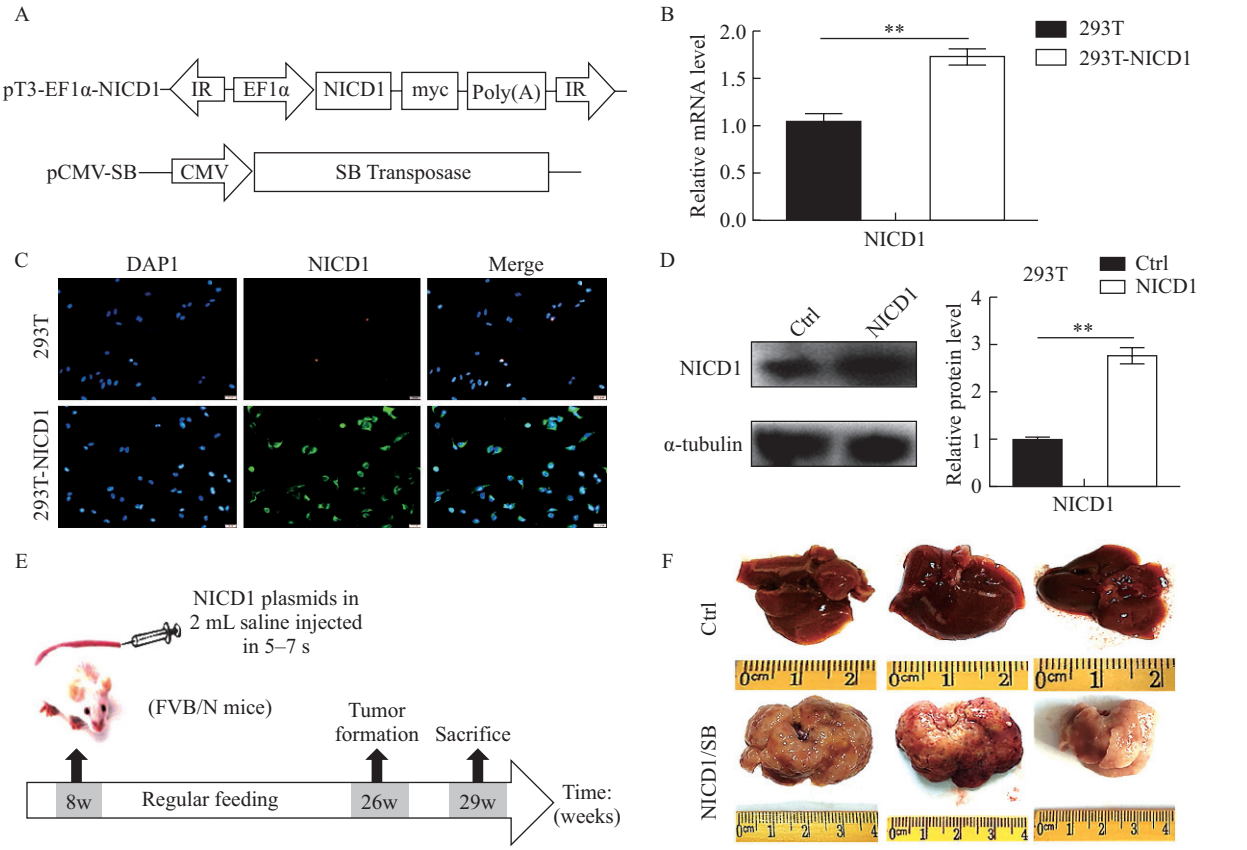

Fig. 2 NICD1-induced primary ICC tumors in mice

A: construction of the NICD1 expression vector pT3-EF1α-NICD1; B–D: NICD1 expression in 293T cells transfected with pT3-EF1α-NICD1. 293T cells were transfected with the empty vector (Ctrl) or pT3- EF1α-NICD1, and the levels of NICD1 were determined by qPCR (B), immunofluorescence (C) and Western blotting (D). E: scheme of the gene delivery strategy through hydrodynamic injection; F: liver phenotype of mice injected with NICD1 or empty vector. Data represent the mean ± SEM of three independent experiments. $^{**}P<0.01$

signaling was involved in ICC tumor formation.

2.5 Inhibition of Notch1 Blocked Cell Proliferation and Induced Apoptosis in ICC Cells

To further explore the role of Notch1 in cell proliferation and tumor formation, we used siRNA to silence Notch1 expression in QBC-939 and RBE cells. Forty-eight h after transfection, Western blotting confirmed the effects of Notch1 silencing (fig. 5A). Notably, silencing Notch1 led to shrinkage of cell membrane and round shapes of cells (fig. 5B). Colony formation assays indicated that the ability of ICC cells to form clones was inhibited after Notch1 silencing (fig. 5C). Additionally, analysis of cell growth indicated that cell proliferation was inhibited in Notch1-silenced cells compared with control cells (fig. 5D). Flow cytometry analysis showed that silencing of Notch1 increased apoptosis by 28% and 36% in QBC-939 and RBE cells, respectively, compared with control (fig. 5E).

2.6 Inhibition of Notch1 Blocked Cell Proliferation and Induced Apoptosis by Activating Phosphatase and Tensin Homolog (PTEN) and p53

To explore the action mechanism of Notch1 on cell cycle and apoptosis, we examined some markers of cell apoptosis. Results of qPCR indicated that p53 and Bax levels were increased upon Notch1 silencing (fig. 6A and 6B). Furthermore, the expression levels of the apoptosis related proteins B-cell lymphoma 2 (Bcl2)-associated X (Bax) and cleaved-caspase 3 were increased and the expression of Bcl2 was reduced (fig. 6C and 6D). These results indicated that Notch1 promoted cell proliferation and inhibited apoptosis in ICC cells.

The PTEN/mouse double minute 2 homolog (MDM2)/p53 signaling pathway plays an important role in cell proliferation. Thus, we examined whether changes in Notch1 levels would affect this signaling. Western blotting data showed that silencing of Notch1 reduced Hes1 levels, and increased PTEN levels. Correspondingly, MDM2 levels decreased and p53 levels increased (fig. 6C). These results suggested that Notch1 maintained the ICC cell survival and growth by activating Hes1, and subsequently inhibiting the PTEN/MDM2/p53 signaling (fig. 6E).

3 DISCUSSION

In the present study, we found, by using the GEO

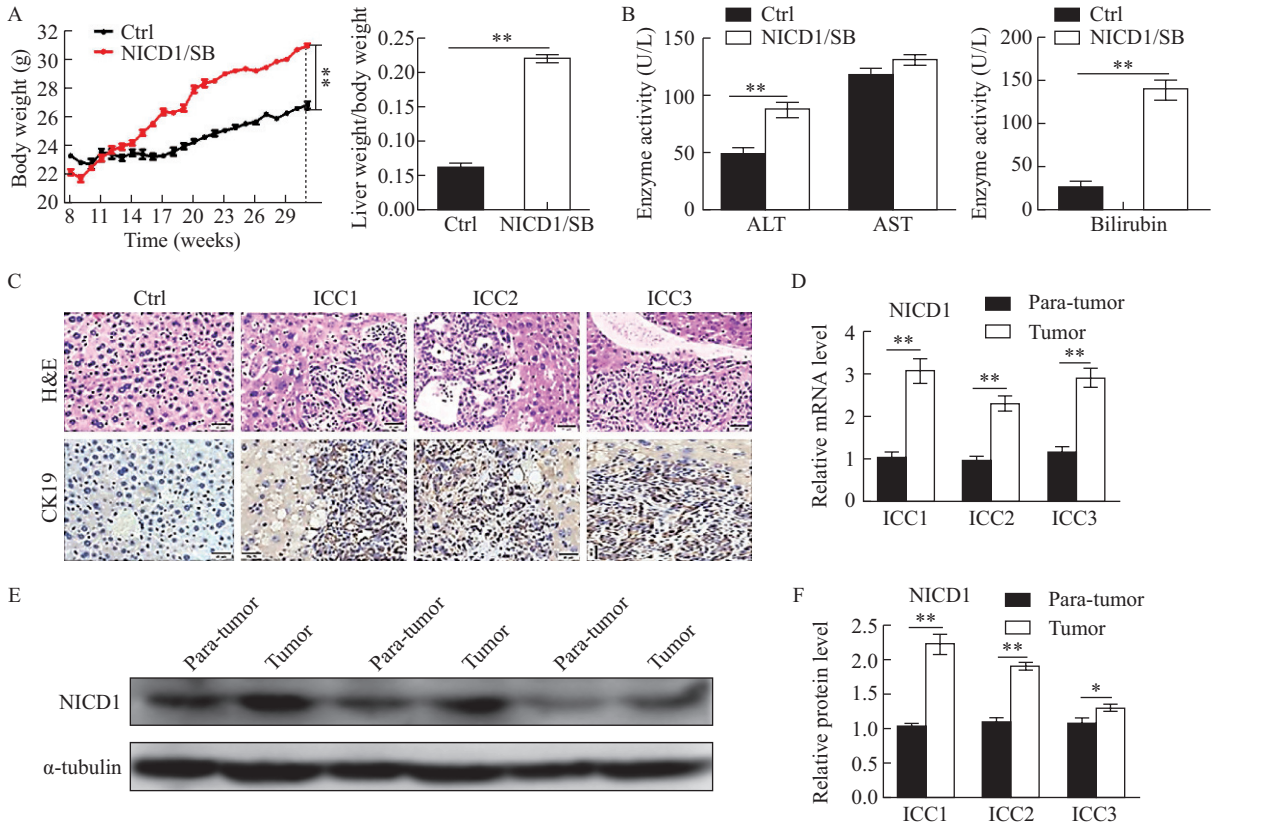

Fig. 3 Characterization of NICD1-induced ICC in FVB/N mice

A: body weight curve and liver weight/body weight ratio of control and ICC mice; B: ALT, AST and bilirubin concentrations in control and ICC mice; C: H&E staining and immunohistochemical staining for CK19 in ICC tissues (magnification, ×200); D and E: expression of NICD1 in tumor tissues and adjacent non-tumor tissues by qPCR (D) and Western blotting (E); F: quantification of the expression of NICD1 in tumor tissues. Data represent the mean ± SEM of three independent experiments. $^{*}P<0.05$, $^{**}P<0.01$

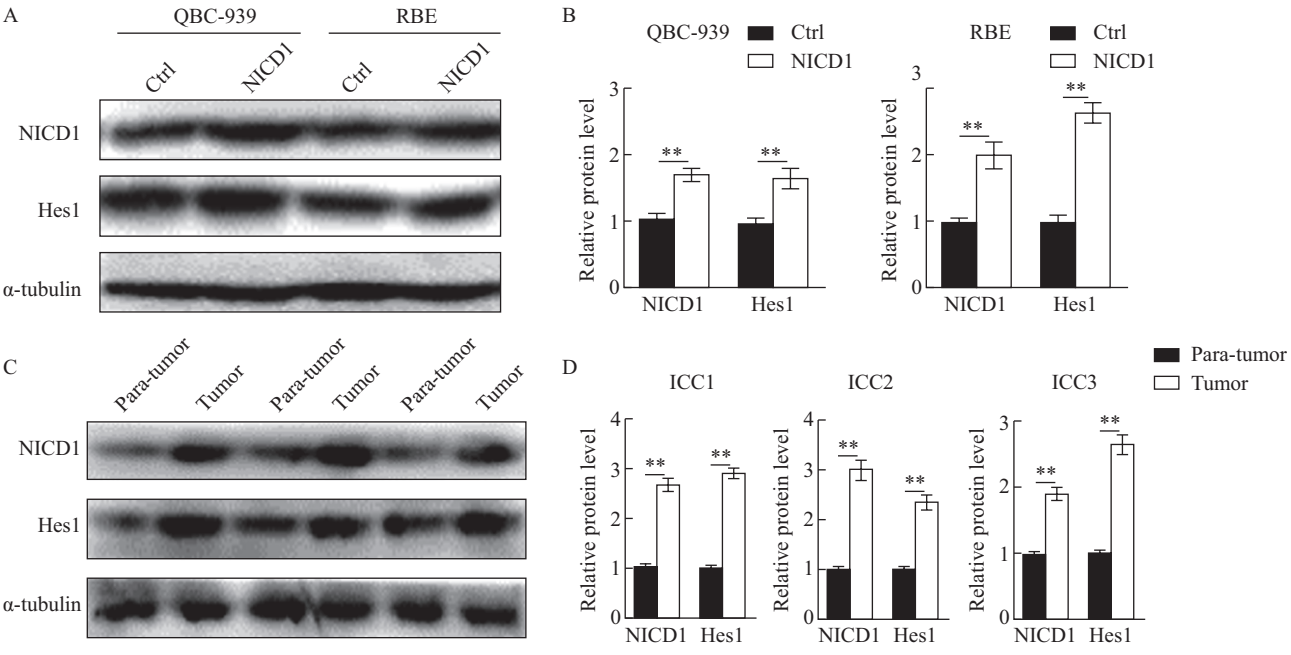

Fig. 4 NICD1 activated Hes1 in human ICC cells and mouse ICC tissues.

A: protein levels of NICD1 and Hes1 detected in QBC-939 and RBE cells transfected with NICD1 or control cells (Ctrl) by Western blotting; B: quantification of the Western blotting results; C: protein levels of NICD1 and Hes1 detected in ICC and adjacent tissues from mice injected with NICD1 by Western blotting; D: quantification of protein levels of NICD1 and Hes1. Data represent the mean ± SEM of three independent experiments. $^{**}P<0.01$

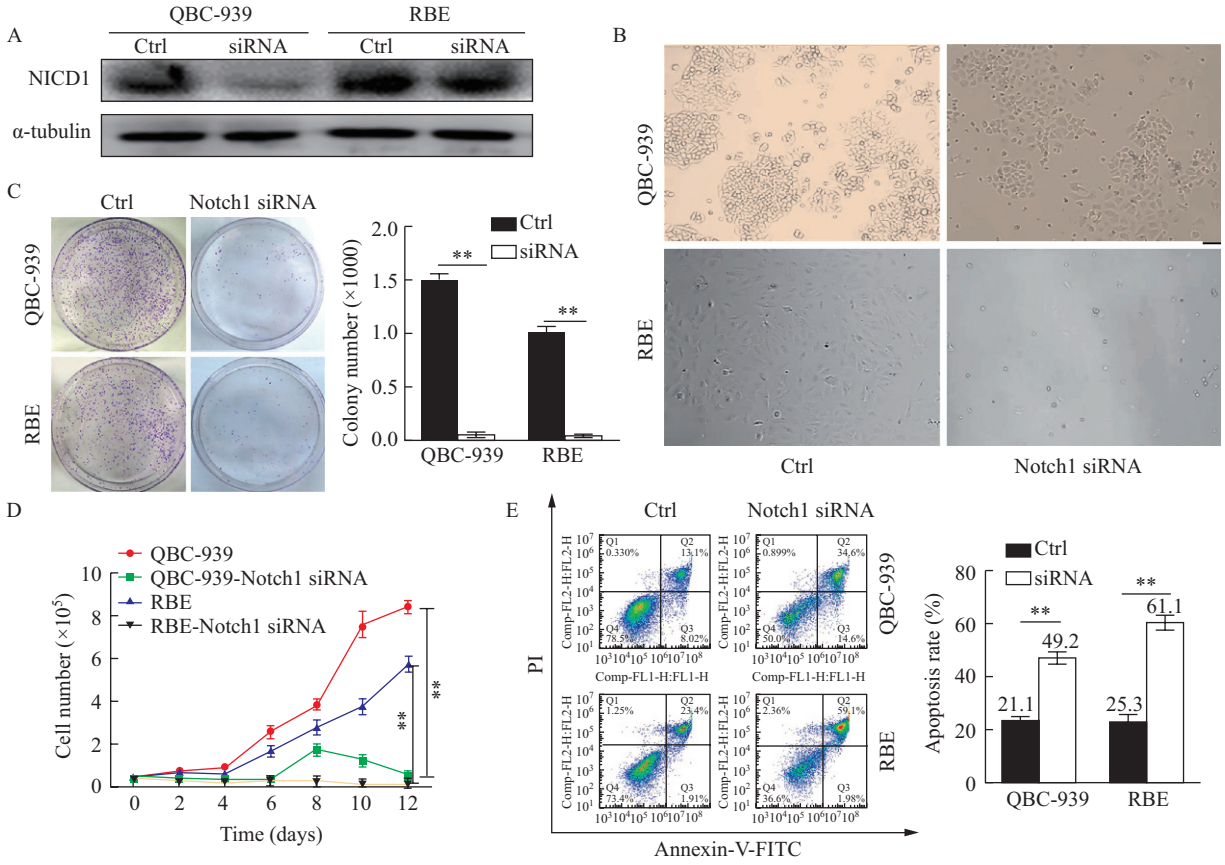

Fig. 5 Knockdown of Notch1 inhibited human ICC cell growth.
A: expression of Notch1 in ICC cells transfected with Notch1 siRNA or scramble siRNA; B: morphology of QBC-939 and RBE cells transfected with Notch1 siRNA and scramble siRNA (magnification, ×200). C: clone formation in ICC cells transfected with Notch1 siRNA or scramble siRNA; D: the number of cells transfected with Notch1 siRNA or scramble siRNA at different time points; E: apoptosis of ICC cells treated with Notch1 siRNA or scramble siRNA by flow cytometry

database, that Notch1 was overexpressed in most ICC samples, which indicated its potential oncogenic role in ICC. Additionally, we found that the expression of Notch1 was higher in tumors tissues than in adjacent non-tumor tissues in samples from ICC patients. Accumulating evidence suggests that the Notch1 signaling pathway is associated with hematological malignancies and the development of many solid tumors, as well as with angiogenesis, neurogenesis and homeostasis[13, 14]. However, Notch1 expression and function in ICC has seldom been reported. Using the public database and clinical samples, we confirmed that Notch1 is highly expressed in human ICC and may play an important role in the development of ICC.

Our study found that injection of NICD1 generated ICC formation in mouse livers. Hydrodynamic gene delivery is an efficient tool to investigate the function of a gene in the liver diseases, especially for live cancer. Using this efficient technique, we successfully transfected NICD1 into mouse livers and observed the formation of primary ICC. Histological analysis confirmed that the tumor induced by NICD1 was ICC, confirming the oncogenic role of Notch1 in ICC formation. Fan *et al* reported that NICD1 plus Akt could induce ICC, but single NICD1 did not[24]. Considering the low transfection efficiency of hydrodynamic injection, we increased the dose of plasmid to 25 μg for the hydrodynamic injection, instead of 5 μg plasmids used in their study. We successfully established the ICC model, and clearly demonstrated that NICD1 could induce ICC by itself in mice, which suggested the critical and robust role of Notch1 signaling in ICC formation.

Notch has been reported to be implicated in many types of cancers, such as leukemia[25, 26], lung adenoma[27], esophageal adenocarcinoma[28], breast cancer[29] and HCC[30]. It has been also revealed that Notch can suppress tumor formation or progression in cervical cancer[31] and B-cell malignancy[32]. Actually, the role of Notch signaling is remarkably varied depending on signal dose and cell context[33]. In this study, our data supported the oncogenic role of Notch in ICC formation and development. Ectopic expression of Notch1 could induce tumor formation by itself in mouse liver, whereas blockade of Notch1 inhibited ICC development. Thus, our study indicated that targeting

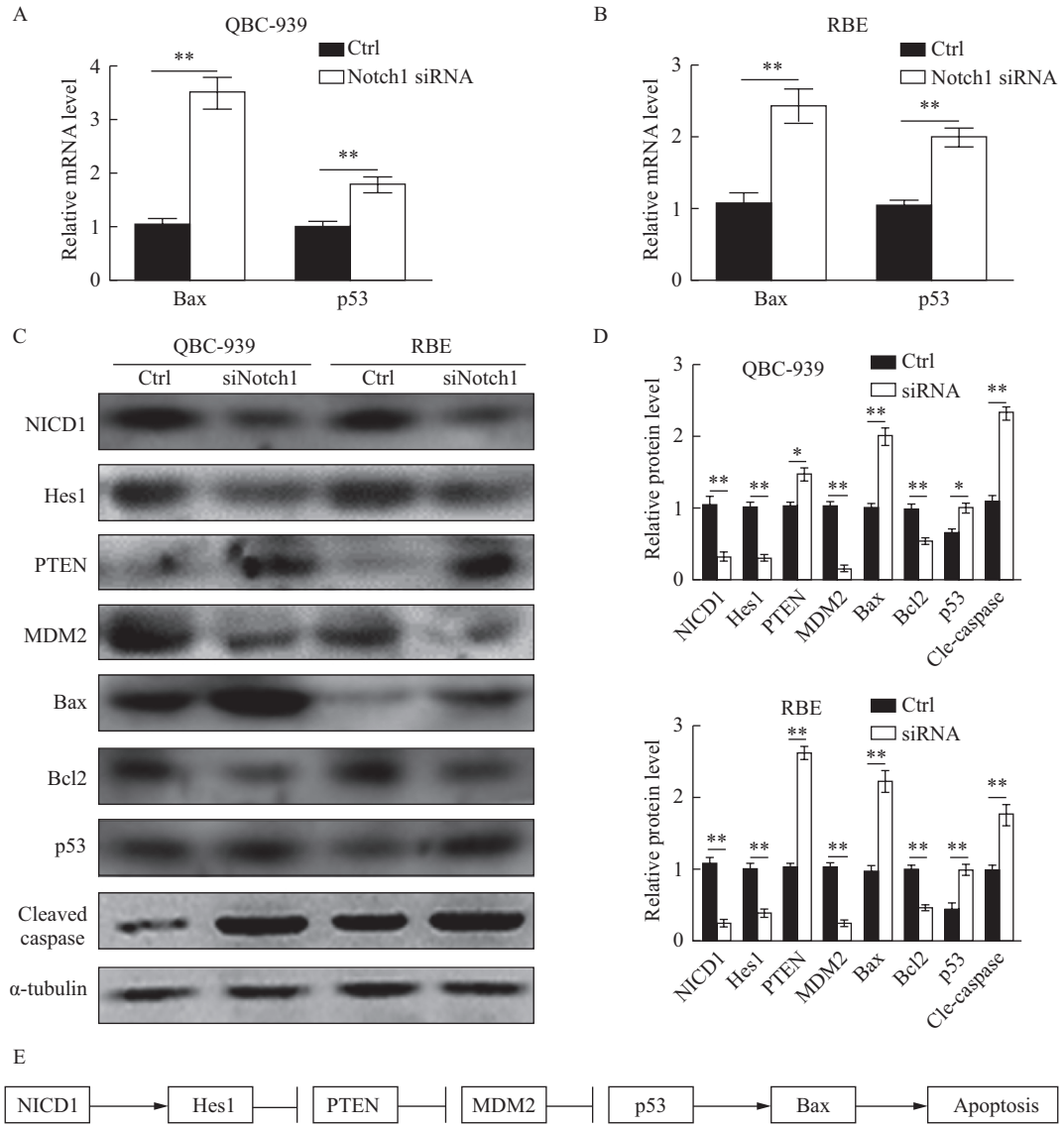

Fig. 6 Knockdown of Notch1 inhibited human ICC cell growth via the PTEN/MDM2/p53 signaling.
A and B: the mRNA level of Bax and p53 in Notch1-silenced QBC-939 cells (A), RBE cells (B) and control cells, detected by qPCR; C: expression of NICD1, Hes1, PTEN, MDM2, Bax, Bcl2, p53 and cleaved caspase in Notch1-silenced or control cells determined by Western blotting; D: quantification of the Western blot results; E: speculation of the signaling pathway of Notch1 in ICC. In the histograms, data represent the mean ± SEM of three independent experiments. $^{*}P<0.05$, $^{**}P<0.01$

Notch signaling would be a potential strategy for ICC treatment.

Notch signaling was documented to drive carcinogenesis by regulating p27cip1/waf1, cyclinD1, c-Myc, p21, Survivin, Slug and Nanog, as well as the nuclear factor-kappa B (NF-κB) pathway[22]. Notch was also found to accelerate cancer formation by promoting epithelial-mesenchymal transition[34]. In this study, we further investigated the action mechanism of Notch1 in ICC. We found that Notch1 induced and maintained ICC growth by repressing PTEN/MDM2/p53 pathway, and hence blocked cell apoptosis and enhanced cell proliferation. When Notch1 was silenced, NICD1 and Hes1 were also inhibited. Notably, inhibition of Hes1 resulted in the activation of PTEN and inhibition of MDM2. MDM2 inhibition activated p53, which induced apoptosis in ICC cells. These data highlights the importance of PTEN/MDM2/p53 pathway in ICC driven by Notch1 signaling. In addition, blocking Notch1 using siRNA also demonstrated the dependence of ICC cells on Notch1 signaling, indicating that the Notch1 or NICD could be used as a treatment target for ICC.

In summary, our data showed the role of Notch1 in ICC and identified a possible novel target for ICC therapy. We believe that inhibition of the Notch1 pathway may be beneficial to ICC patients. Additional studies are necessary to address this possibility.

Conflict of Interest Statement

The authors declare that they have no conflict of interest.

REFERENCES

1 Zhao Q, Yu WL, Lu XY, *et al*. Combined hepatocellular and cholangiocarcinoma originating from the same clone: a pathomolecular evidence-based study. Chin J Cancer, 2016,35(1):82-90
2 Razumilava N, Gores GJ. Classification, diagnosis, and management of cholangiocarcinoma. Clin Gastroenterol Hepatol, 2013,11(1):13-21
3 Razumilava N, Gores GJ. Cholangiocarcinoma. Lancet, 2014:2168-2179
4 Wang FS, Fan JG, Zhang Z, *et al*. The global burden of liver disease: the major impact of China. Hepatology, 2014,60(6):2099-2108
5 Esnaola NF, Meyer JE, Karachristos A, *et al*. Evaluation and management of intrahepatic and extrahepatic cholangiocarcinoma. Cancer, 2016,122(9):1349-1369
6 Papatheodoridis GV, Lampertico P, Manolakopoulos S, *et al*. Incidence of hepatocellular carcinoma in chronic hepatitis B patients receiving nucleos(t)ide therapy: a systematic review. J Hepatol, 2010,53(2):348-356
7 Alves RC, Alves D, Guz B, *et al*. Advanced hepatocellular carcinoma: Review of targeted molecular drugs. Ann Hepatol, 2011,10(1):21-27
8 Belina F. Hilar cholangiocarcinoma (Klatskin tumor) - current treatment options. Rozhl Chir, 2013,92:4-15
9 Yu Y, Wang L, Tang W, *et al*. RNA interference-mediated knockdown of Notch-1 inhibits migration and invasion, down-regulates matrix metalloproteinases and suppresses NF-kappaB signaling pathway in trophoblast cells. Acta Histochem, 2014,116(5):911-919
10 Pupo M, Pisano A, Abonante S, *et al*. GPER activates Notch signaling in breast cancer cells and cancer-associated fibroblasts (CAFs). Int J Biochem Cell Biol, 2014,46:56-67
11 Dahan S, Rabinowitz KM, Martin AP, *et al*. Notch-1 signaling regulates intestinal epithelial barrier function, through interaction with CD4+ T cells, in mice and humans. Gastroenterology, 2011,140:550-559
12 Jensen J, Pedersen EE, Galante P, *et al*. Control of endodermal endocrine development by Hes-1. Nat Genet, 2000,24(1):36-44
13 Sun YY, Li L, Liu XH, *et al*. The spinal notch signaling pathway plays a pivotal role in the development of neuropathic pain. Mol Brain, 2012,5:23-32
14 Takebe N, Nguyen D, Yang SX. Targeting notch signaling pathway in cancer: clinical development advances and challenges. Pharmacol Ther, 2014,141(2):140-149
15 Wolpin BM, Mayer RJ. A step forward in the treatment of advanced biliary tract cancer. N Engl J Med, 2010,362(14):1335-1337
16 Binato M, Schmidt MK, Volkweis BS, *et al*. Mouse model of diethylnitrosamine-induced gastric cancer. J Surg Res, 2008,148(2):152-157
17 Yang H, Li TW, Peng J, *et al*. A mouse model of cholestasis-associated cholangiocarcinoma and transcription factors involved in progression. Gastroenterology, 2011,141(1): 378-388
18 Ju HL, Han KH, Lee JD, *et al*. Transgenic mouse models generated by hydrodynamic transfection for genetic studies of liver cancer and preclinical testing of anti-cancer therapy. Int J Cancer, 2016,138(1):1601-1608
19 Calvisi DF, Wang C, Ho C, *et al*. Increased lipogenesis, induced by AKT-mTORC1-RPS6 signaling, promotes development of human hepatocellular carcinoma. Gastroenterology, 2011,140(3):1071-1083
20 Chen X, Calvisi DF. Hydrodynamic transfection for generation of novel mouse models for liver cancer research. Am J Pathol, 2014,184(4):912-923
21 Wang Y , Wang Y, Zhang L, *et al*. Endonuclease Restriction-Mediated Real-Time Polymerase Chain Reaction: A Novel Technique for Rapid, Sensitive and Quantitative Detection of Nucleic-Acid Sequence. Front Microbiol, 2016,7:1104-1114
22 Yuan X, Wu H, Xu H, *et al*. Notch signaling: an emerging therapeutic target for cancer treatment. Cancer Lett, 2015,369(1):20-27
23 Kopan R, IIagan MX. The canonical Notch signaling pathway: unfolding the activation mechanism. Cell, 2009,137(2):216-233
24 Fan B, Malato Y, Calvisi DF, *et al*. Cholangiocarcinomas can originate from hepatocytes in mice. J Clin Invest, 2012,122(8):2911-2915
25 O'Neil J, Calvo J, McKenna K, *et al*. Activating Notch1 mutations in mouse models of T-ALL. Blood, 2006,107(2):781-785
26 Yan XQ, Sarmiento U, Sun Y, *et al*. A novel Notch ligand, Dll4, induces T-cell leukemia/lymphoma when overexpressed in mice by retroviral-mediated gene transfer. Blood, 2001,98(13):3793-3799
27 Allen TD, Rodriguez EM, Jones KD, *et al*. Activated Notch1 induces lung adenomas in mice and cooperates with Myc in the generation of lung adenocarcinoma. Cancer Res, 2011,71(18):6010-6018
28 Wang Z, Da Silva TG, Jin K, *et al*. Notch signaling drives stemness and tumorigenicity of esophageal adenocarcinoma. Cancer Res, 2014,74(21):6364-6374
29 Gallahan D, Callahan R. The mouse mammary tumor associated gene INT3 is a unique member of the NOTCH gene family (NOTCH4). Oncogene, 1997,14(16):1883-1890
30 Dill MT, Tornillo L, Fritzius T, *et al*. Constitutive Notch2 signaling induces hepatic tumors in mice. Hepatology, 2013,57(4):1607-1619
31 Talora C, Sgroi DC, Crum CP, *et al*. Specific down-modulation of Notch1 signaling in cervical cancer cells is required for sustained HPV-E6/E7 expression and late steps of malignant transformation. Genes Dev, 2002,16(17):2252-2263
32 Zweidler-McKay PA, He Y, Xu L, *et al*. Notch signaling is a potent inducer of growth arrest and apoptosis in a wide range of B-cell malignancies. Blood, 2005,106(12): 3898-3906
33 Aster JC, Pear WS, Blacklow SC. The Varied Roles of Notch in Cancer. Annu Rev Pathol, 2017,12:245-275
34 Bolos V, Grego-Bessa J, de la Pompa JL. Notch signaling in development and cancer. Endocr Rev, 2008,28(3): 339-363

(Received Feb. 19, 2019; revised Sep. 2, 2019)